Electrically controlled entanglement of cavity photons with electromagnons

Z. Toklikishvili,[1] L. Chotorlishvili [ORCID],[2,3] R. Khomeriki [ORCID],[1] V. Jandieri [ORCID],[3,4] and J. Berakdar [ORCID][3]

[1]*Faculty of Exact and Natural Sciences, Tbilisi State University, Chavchavadze av.3, 0128 Tbilisi, Georgia*
[2]*Department of Physics and Medical Engineering, Rzeszów University of Technology, 35-959 Rzeszów, Poland*
[3]*Institut für Physik, Martin-Luther-Universität Halle-Wittenberg, D-06099 Halle, Germany*
[4]*General and Theoretical Electrical Engineering (ATE), Faculty of Engineering, University of Duisburg-Essen
and CENIDE - Center for Nanointegration Duisburg-Essen, D-47048 Duisburg, Germany*

Electromagnonics is an emerging field with a focus on entangling magnonic excitations to the microwave cavity photon modes with the prospect for use in quantum information science. Here, we discuss a class of Hamiltonians that embody a substantial steady-state photon-magnon entanglement enabled by a chiral coupling of the magnonic system to the cavity electric field. It is demonstrated how the entanglement can be controlled via external parameters. As a realization, we study a layered system that hosts an interfacial Dzyaloshinskii-Moriya interaction whose strength varies linearly with the cavity electric field rendering the low-energy spin excitations susceptible to an electric field and resulting in nonlinear magnon-photon dynamics. Accounting for interactions with the environment, we derive from the stochastic quantum Langevin equations explicit expressions evidencing the existence of a finite, steady-state entanglement and detailing its dependencies on external probes. The results point to particular types of electromagnonic systems that are potentially useful for quantum information applications.

I. INTRODUCTION

Recent advances in quantum devices have rendered possible the experimental implementation of theoretical concepts for quantum metrology. Established research schemes exploit the cavity quantum electrodynamics to enable atom-photon entanglement or enhanced photon-phonon interactions in optonanomechanical systems [1–5]. Relatively recent developments are the fields of electromagnonics [6] and optomagnonics [7–10] which refer to studies on magnetically ordered systems in photonic cavities with the aim to increase and functionalize the coupling of the cavity and optical photons to low-energy magnetic excitations, for example, spin waves (with magnons being the quanta of these excitations). For a range of materials including ferrimagnet, antiferromagnet, or helical multiferroic such as Cu_2OSeO_3 [11–19] a coupled magnon-photon dispersion and energy levels repulsion due to magnon-photon modes hybridization were found. Level repulsion or attraction of classical modes does not imply an underlying quantum information content. From a quantum information point of view, interaction does not guarantee a steady-state entanglement of these two (magnon and photon) bosonic continuous modes [20–22].

We will demonstrate that, for a steady-state entanglement [23,24] that survives environmental perturbations, the system must involve certain type of interactions leading to a nonlinear response of the coupled modes. For a potential use in quantum information circuits, it is important to achieve a sizable photon-magnon entanglement that can be controlled by external fields. We demonstrate the need to go beyond the conventional optomagnonic setup to entangle and

control the photon and magnon modes, and present a proposal based on feasible materials for entangled (electro)magnonics. Reference [25] demonstrated that a steady-state tripartite entanglement of a photon-magnon-phonon system in the presence of noise can be obtained. Here we show that introducing Dzyaloshinskii-Moriya interactions (DMI) and applying a static electric field, even bipartite photon-magnon systems could exhibit feasible entanglement effect in the presence of noise.

We exploit the experimental observation (backed and rationalized with theoretical simulations) that layered systems containing an ultrathin magnetic film exhibit an interfacial DMI with an electrically tunable strength. Examples are Co films sandwiched between nonmagnetic layers [26] or MgO/Fe/Pt [27] (cf. Fig. 1). In fact, the low-energy excitations are then electromagnons, as detailed below. The susceptibility of the spin excitations to an electric field (mediated by DMI) offers the opportunity of entangling the spin modes to the cavity electric field. In contrast to conventional magnonics where the cavity magnetic field interacts with the magnon modes, the setup sketched in Fig. 1 is demonstrated to exhibit a nonlinear spin dynamic and a sizable steady-state electromagnon-photon entanglement that can be varied by the cavity characteristics and/or an electric gate.

Paper is organized as follows. In Sec. II, we consider magnetoelectric excitations in the cavity and specify the models of interest, in Sec. III, we demonstrate absence of the steady-state magnon-photon entanglement in the conventional model. In Sec. IV, we analyze the role of the DMI term in the formation of robust magnon-photon entanglement. In Sec. V, we discuss experimental proposals
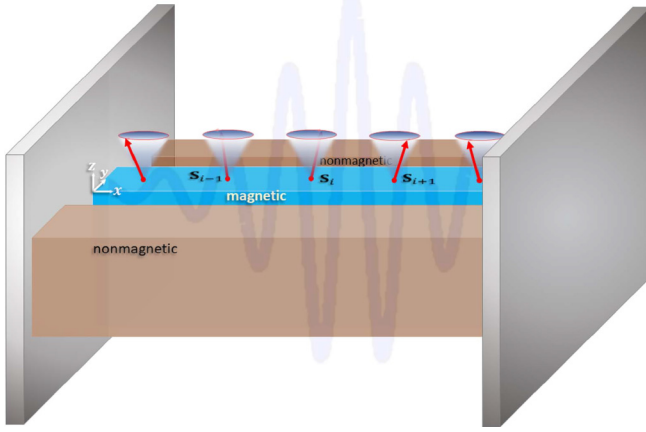
FIG. 1. Setup for photon-magnon entanglement. A cavity field is coupled to magnonic excitations in a ferromagnetic layer which is sandwiched between nonmagnetic layers resulting in an electrically tunable interfacial Dzyaloshinskii-Moriya interaction (DMI). The DMI mediates a coupling of the cavity electric field to magnetic excitations. An external static magnetic field is applied along the z axis. The cavity field is linearly polarized along the y direction.

for measuring the robust steady-state magnon-photon entanglement. Technical details of calculations are presented in Appendices (A–C).

II. CAVITY MAGNETOELECTRIC EXCITATIONS

Our aim is to deduce material and system-independent trends and statements on the entanglement existence and its dependencies. To be specific however, we refer to Fig. 1 as the cavity-enclosed layered heterostructure. The DMI vector is along the z axis. As evidenced by theory and experiment [26], the DMI strength depends linearly on the magnitude of an electric field along the interfacial direction y. A relatively small perpendicular magnetic anisotropy [26] exists but it is negligibly small as compared to the DMI strength.

The cavity field (cf. Fig. 1) is described by $\hat{\mathcal{E}} = \sum_l i\epsilon \mathbf{U}_l(\mathbf{r})(\hat{a}_l - \hat{a}_l^{\dagger})$, $\hat{\mathbf{h}} = \sum_l \epsilon \mathbf{U}_l^h(r)(\hat{a}_l + \hat{a}_l^{\dagger})$ where $\hat{a}_l$ and $\hat{a}_l^{\dagger}$ are annihilation and creation operators of photons of the mode l, respectively. Below, we study a field with fixed frequency ω_f and polarized along the y axis (which fixes l). $\epsilon = \sqrt{\frac{\omega_f}{2\varepsilon_0 V}}$, where $\omega_f = c|k|$ is the energy dispersion and k is the wave vector (c is light speed). V is the cavity mode volume, ε_0 is the vacuum permittivity, and $\mathbf{U}(\mathbf{r})$, $\mathbf{U}_l^h(r)$ are the cavity mode function for photon electric and magnetic fields. The components of the cavity mode function follow from the Helmholtz equation $\triangle U_{x,y,z} + k^2 U_{x,y,z} = 0$.

As control parameters, we apply an external (unquantized) static electric field E_{0y} along the y direction and a strong magnetic field H_0 along the z direction. The spins in the magnetic layer experience a DMI with a strength D_0 related to an intrinsic DMI part, and a part controllable by E_{0y} which behaves as $D_{0z} = \alpha E_{0y}$. A further DMI contribution, proportional to α depends on the quantized cavity electric field $\hat{\mathcal{E}}$. The linear dependence of DMI on the electric fields is evi-

denced by theory and experiment [26] yielding an estimate of the (magnetoelectric) coupling constant α.

The low-energy spin dynamics of the system sketched in Fig. 1 is captured by the Hamiltonian

$$\hat{H} = -J \sum_n \hat{\mathbf{S}}_n \hat{\mathbf{S}}_{n+1} - H_0 \sum_n \hat{S}_n^z + \mathcal{B}\hat{S}_n^{\perp} e^{-i(\omega_0 t - kx)}$$
$$+ (D_0 + D_{0z}) \sum_n (\hat{\mathbf{S}}_n \times \hat{\mathbf{S}}_{n+1})_z + \hat{H}_c \quad (1)$$

with

$$\hat{H}_c = \omega_f \hat{a}^+ \hat{a} - \sum_n \hat{\mathbf{h}} \cdot \hat{\mathbf{S}}_n + \alpha \hat{\mathcal{E}}_y \sum_n (\hat{\mathbf{S}}_n \times \hat{\mathbf{S}}_{n+1})_z.$$

Here $\hat{S}_n^{\perp} = \hat{S}_n^x + i\hat{S}_n^y$. The electric $\hat{\mathcal{E}}$ and magnetic $\hat{\mathbf{h}}$ components of the cavity field are to be expressed through the photon creation and annihilation operators $\hat{a}^+$ and $\hat{a}$. $\hat{\mathbf{S}}_n$ describes the spin on the nth site exchange coupled (with coupling constant $J > 0$) to the next neighbor (sample's translational invariance along z is assumed). In Eq. (1), $\hat{H} - \hat{H}_c$ describes an exchange-coupled spin system with DMI in static electric and magnetic fields and circularly polarized magnetic field $\mathcal{B}$, while $\hat{H}_c$ encompasses the cavity fields coupled to the spins. The last term in $\hat{H}_c$ is a product of three operators which we show to result in a nonlinear spin wave dynamics and a finite steady-state, electrically sensitive magnon-photon entanglement. For $\alpha = 0$ (thus $D_{0z} = \alpha E_{0y} = 0$), we retrieve the conventional cavity photon magnon Hamiltonians [18] (with or without DMI), which leads in first order to a linear dynamic and a vanishing steady-state entanglement.

To account for environmental effects, we introduce $\hat{a}_{\text{in}}(t)$ and $\hat{m}_{k,\text{in}}(t)$ as input noise operators affecting the cavity and magnon modes, respectively. The noise is characterized by the following correlators [25]: $\langle a_{\text{in}}(t)a_{\text{in}}^+(t')\rangle = [N_a(\omega_f) + 1]\delta(t - t')$, $\langle a_{\text{in}}^+(t)a_{\text{in}}(t')\rangle = N_a(\omega_f)\delta(t - t')$, $\langle m_{k,\text{in}}(t)m_{k,\text{in}}^+(t')\rangle = [N_m(\omega_k) + 1]\delta(t - t')$, $\langle m_{k,\text{in}}^+(t)m_{k,\text{in}}(t')\rangle = N_m(\omega_k)\delta(t - t')$, $N_a(\omega_f) = [\exp[(\hbar\omega_f/k_B T)] - 1]^{-1}$, and $N_m(\omega_k) = [\exp[(\hbar\omega_k/k_B T)] - 1]^{-1}$ (and T is the temperature). Upon a Holstein-Primakoff transformation [28] we switch to reciprocal space operators $\hat{m}_k^+$ and $\hat{m}_k$, and proceed in the spirit of the input-output formalism [12,29–31] to obtain a set of quantum Langevin equations for the photon and magnon modes affected by the magnon and photon baths ($\gamma_{f/m}$ are photonic/magnonic damping rates):

$$\frac{d\hat{a}(t)}{dt} = -i[\hat{a}(t), \hat{H}] - \gamma_f \hat{a}(t) + \sqrt{2\gamma_f}\hat{a}_{\text{in}}(t),$$
$$\frac{d\hat{m}_k(t)}{dt} = -i[\hat{m}_k(t), \hat{H}] - \gamma_m \hat{m}_k(t) + \sqrt{2\gamma_m}\hat{m}_{k,\text{in}}(t). \quad (2)$$

The procedure applies to both, the conventional ($\alpha = 0$, $D_0 \neq 0$) and our general ($\alpha \neq 0$) cases.

For clarity, we use dimensionless time by redefining $t \to \gamma S_0 J t$. The DMI constants, excitation frequencies, and damping rates are measured in units of $\gamma S_0 J$, where γ is the gyromagnetic ratio, and S_0 is the saturated spin value. The experimental parameters, the symmetric and antisymmetric exchange constants are taken from Refs. [32] and [26], respectively. The exchange constant per magnetic atom is chosen to be $JS_0^2 \approx 5$ meV, while the enhanced DMI constant per

atom is of the order of 1.55 meV. We use the value of D_0 in units of J as $D_0 = 0.3$. The parameter α quantifies the linear dependence of the DMI constant on the value of the external electric field and is equal to $\alpha \approx 20$ meV nm V^{-1}. For an electric field in the range of 1 V/nm, the values of D_{0z} and $D = \epsilon U \alpha$ are about 0.05 (in units of J), while the circularly polarized magnetic field strength $\mathcal{B}$ is measured in units of JS_0 and its values are on the order 0.01 A/nm.

III. CONVENTIONAL CASE - NO ENTANGLEMENT

For $\alpha \to 0$; or if $\alpha \neq 0$ but the electric fields (static or cavity fields) are not directed along y axis, our problem reduces to the conventional optomagnonic Hamiltonian $\hat{H}_{\alpha=0}$ [18]. In rotating wave approximation, Eq. (1) reduces for linear spin excitations to

$$\hat{H}_{\alpha=0} = \sum_{f,k} \omega_k \hat{m}_k^+ \hat{m}_k + \omega_f \hat{a}_f^+ \hat{a}_f + g(\hat{m}_k^+ \hat{a}_f + \hat{m}_k \hat{a}_f^+), \quad (3)$$

where ω_k and ω_f are spectra of the magnon and photon subsystems, and the magnonic spectrum has the form

$$\omega_k = H_0 + (1 - \cos k) + D_0 \sin k, \quad (4)$$

where g is the coupling to the cavity magnetic field. In (3), for brevity we dropped the magnonic pump field $\mathcal{B}$, however it is included in the calculations and has a crucial importance for the case $\alpha \neq 0$.

In the conventional model (3), the magnon-photon entanglement is zero. In the absence of the environmental effects for model $\hat{H}_{\alpha=0}$, one can calculate the magnon-photon entanglement in the eigenstates of $\hat{H}_{\alpha=0}$ and the entanglement between the cavity field and the coherent magnon state. The Hamiltonian $\hat{H}_{\alpha=0}$ conserves the mean excitation number in the system $n_\beta + n_{ph} = $ const, where n_β and n_{ph} are magnon and photon numbers, respectively. At first we assume that the number of magnons and photons is very small (e.g., zero or single magnon and photon states $n_\beta = 0, 1$ and $n_{ph} = 0, 1$). Then using the basis of uncoupled magnon $|\beta\rangle_m$ and photon $|\alpha\rangle_f$ states $|\beta\rangle_m \otimes |\alpha\rangle_f$, we diagonalize $\hat{H}_{\alpha=0}$ and find the eigenstates $|\Psi\rangle_n$ and eigenvalues E_n, $n = 1, \dots, 4$ of the Hamiltonian $\hat{H}_{\alpha=0}$. The two entangled states

$$|\Psi\rangle_{1,2} = A|0\rangle_m \otimes |1\rangle_f \pm B|1\rangle_m \otimes |0\rangle_f, \quad (5)$$

(the functions A and B are given below explicitly) have the same concurrence and the other two $|\Psi\rangle_{3,4}$ are product states (not shown). Considering only entangled states $|\Psi\rangle_1$ or $|\Psi\rangle_2$ we construct the density matrices $\hat{\rho}_n = |\Psi\rangle\langle\Psi|_{n=1,2}$ and calculate the magnon-photon concurrence:

$$C_n = \max(0, \sqrt{R_{n,1}} - \sqrt{R_{n,2}} - \sqrt{R_{n,3}} - \sqrt{R_{n,4}}), \quad (6)$$

where $R_{n,i}$ are the eigenvalues of the matrix $R_n = \hat{\rho}_n(\hat{\sigma}_1^y \otimes \hat{\sigma}_2^y)(\hat{\rho}_n)^*(\hat{\sigma}_1^y \otimes \hat{\sigma}_2^y)$ in decreasing order calculated in the computational basis $|\beta\rangle_m \otimes |\alpha\rangle_f$, α, $\beta = 0, 1$. The explicit expression of the concurrence reads

$$C_{|\Psi\rangle} = \frac{2g}{\sqrt{(\omega_k - \omega_f)^2 + 4g^2}}. \quad (7)$$

The concurrence is maximal $C_{|\Psi\rangle} = 1$ at resonance $\omega_k = \omega_f$ when the eigenstates correspond to the Bell's state, i.e., $A =$

$B = 1/\sqrt{2}$, $|\Psi\rangle \equiv |\Psi\rangle^+$. In the nonresonant case, the expressions of the coefficients A and B are involved:

$$E = \frac{\omega_k - \omega_f + \sqrt{(\omega_k - \omega_f)^2 + 4g^2}}{2},$$

$$A = \frac{1}{\sqrt{2}} \frac{\sqrt{\omega_f - \omega_k + \sqrt{(\omega_k - \omega_f)^2 + 4g^2}}}{\sqrt[4]{(\omega_k - \omega_f)^2 + 4g^2}},$$

$$B = \frac{\sqrt{2}g}{\sqrt[4]{(\omega_k - \omega_f)^2 + 4g^2} \sqrt{\omega_f - \omega_k + \sqrt{(\omega_k - \omega_f)^2 + 4g^2}}}.$$

While in Eq. (7), entanglement between magnons and photons is not zero, entanglement becomes zero when we consider environmental effect (see below). We proceed with the less trivial case when the number of magnons in the cavity field is larger $n_\beta \gg 1$.

To calculate entanglement between cavity field and coherent magnon states, we follow [33] and solve Schrödinger's equation

$$i\frac{d}{dt}|\psi\rangle = \hat{H}_{\alpha=0}|\psi\rangle, \quad (8)$$

using the following ansatz

$$|\psi(t)\rangle = \sum_{n=0}^{\infty} [\varphi_{f=0,n+1}(t)|f = 0, n+1\rangle$$
$$+ \varphi_{f=1,n}(t)|f = 1, n\rangle] + \varphi_{f=0,0}(t)|f = 0, 0\rangle. \quad (9)$$

Here, f defines the photon number and $|n\rangle$ stands for the magnon coherent state. In the resonant case, the solution of Eq. (8) has the form

$$\varphi_{f=1,n}(t) = C_n w_n c_1 - iS_n w_{n+1} c_0,$$
$$\varphi_{f=0,n+1}(t) = C_n w_{n+1} c_0 - iS_n w_n c_1,$$
$$\varphi_{f=0,0}(t) = c_0 w_0. \quad (10)$$

c_0 and c_1 define the amplitudes of the zero and single photon states, $C_n = \cos(\sqrt{n+1}gt)$, $S_n = \sin(\sqrt{n+1}gt)$, and $w_n^2 = \frac{n_\beta^n}{n!}e^{-n_\beta}$ is the magnon coherent state with the mean magnon number n_β. Taking into account Eq. (10), we construct the reduced density matrix after tracing the magnon states $\hat{\varrho} = \sum_{n=0}^{\infty} \langle n|\psi(t)\rangle\langle\psi(t)|n\rangle$. The entanglement between the cavity field and the coherent magnon states is quantified in terms of purity

$$P = \text{Tr}(\hat{\varrho}^2) = \sum_{n=0}^{\infty} [(|\varphi_{f=1,n}|^2 + |\varphi_{f=0,n+1}|^2)^2 + 2|\varphi_{f=0,0}|^2$$
$$\times (|\varphi_{f=0,n+1}|^2 + |\varphi_{f=1,n}|^2)] + |\varphi_{f=0,0}|^4.$$

Using Eq. (10), from the above equation we infer

$$P = |c_1|^4 e^{-2n_\beta} I_0(2n_\beta) + 2|c_0|^2|c_1|^2 e^{-2n_\beta} I_1(2n_\beta)$$
$$+ |c_0|^4 e^{-2n_\beta}(I_0(2n_\beta) - 2) + 2|c_0|^2 e^{-n_\beta}. \quad (11)$$

$I_n(x)$ is the modified Bessel function. In the limit of a large magnon number $n_\beta \gg 1$, we find $P = 0$, meaning zero entanglement between the quantized cavity field and classical spin wave.

To apply the procedure (2) to Eq. (3), we specify a linear amplifier $\mathcal{A}$ which transforms the input state $\hat{\rho}_{\text{in},n}$ into an output signal $\hat{\rho}_{\text{out}} = \mathcal{A}\hat{\rho}_{\text{in},n}$ and has the following property $\langle \hat{a} \rangle_{\text{out}} = \text{tr}[\hat{a}\mathcal{A}\hat{\rho}_{\text{in}}] = G\langle \hat{a} \rangle_{\text{in}}$. Considering the Hamiltonian $\hat{H}_{\alpha=0}$ given by Eq. (3) in the main text, we solve for the associated Eqs. (2). To this end, we implement the input-output formalism. The output field is calculated from the following equation: $\hat{a}_{\text{out}} + \hat{a}_{\text{in}} = \sqrt{2\gamma_f}\hat{a}$. The amplifier is phase preserving if G is real. Then, for a resonance frequency component at frequency (ω) of the stochastic input field $\hat{a}_{\text{in}}(\omega) = e^{i\omega t}\hat{a}_{\text{in}}$, we seek harmonic solutions of Eqs. (2), i.e., $\hat{a} \sim e^{i\omega t}$ and $\hat{m}_k \sim e^{i\omega t}$. We assume that the magnons are not pumped into the system $\hat{m}_{k,\text{in}} = 0$ and therefore

$$\hat{a}_f = \frac{\sqrt{2\gamma_f}(i(\omega_k - \omega) + \gamma_m)}{(i(\omega_f - \omega) + \gamma_f)(i(\omega_k - \omega) + \gamma_m) + g^2}\hat{a}_{f,\text{in}}. \quad (12)$$

Taking into account $\hat{a}_{\text{out}} + \hat{a}_{\text{in}} = \sqrt{2\gamma_f}\hat{a}$ for the reflection coefficient, we obtain

$$\frac{a_{\text{out}}}{a_{\text{in}}} = \frac{2\gamma_f(i(\omega_k - \omega) + \gamma_m)}{(i(\omega_f - \omega) + \gamma_f)(i(\omega_k - \omega) + \gamma_m) + g^2} - 1. \quad (13)$$

We evaluate the real and imaginary parts and obtain the microwave reflection coefficient in the explicit form:

$$G = \frac{a_{\text{out}}}{a_{\text{in}}} \equiv G_0 e^{i\phi_g}, \quad G_0 = \sqrt{G_1^2 + G_2^2}, \quad \tan\phi_g = \frac{G_2}{G_1},$$

$$G_1 = -\frac{g^4 - 2g^2\omega_m\Theta_f + (\gamma_m^2 + \omega_m^2)(\Theta_f^2 - \gamma_f^2)}{((\gamma_m\gamma_f - \omega_m\Theta_f) + g^2)^2 + (\Theta_f\gamma_m + \omega_m\gamma_f)^2},$$

$$G_2 = -\frac{2\gamma_f\Theta_f(\gamma_m^2 + \omega_m^2) - 2g^2\omega_m\gamma_f}{((\gamma_m\gamma_f - \omega_m\Theta_f) + g^2)^2 + (\Theta_f\gamma_m + \omega_m\gamma_f)^2},$$

$$\omega_m = \omega_k - \omega, \quad \Theta_f = \omega_f - \omega. \quad (14)$$

The amplitude and the phase of the amplifier are plotted in Fig. 2 exhibiting absorption tracks, along which the amplitude of the amplifier is less than one, and the phase abruptly changes sign. For those values of the parameters, the absorption is large.

To study the steady-state magnon-photon entanglement corresponding to $\hat{H}_{\alpha=0}$, we introduce (similar to Refs. [25,34,35]) the following variables (x_m, p_m, x_a, p_a) and the vectors $x_m = (\hat{m} + \hat{m}^+)/\sqrt{2}$, $p_m = i(\hat{m}^+ - \hat{m})/\sqrt{2}$, $x_a = (\hat{a} + \hat{a}^+)/\sqrt{2}$, $p_a = i(\hat{a}^+ - \hat{a})/\sqrt{2}$, $u(t) = [x_m, p_m, x_a, p_a]$, and $n = [\sqrt{2\gamma_f}x_m^{\text{in}}, \sqrt{2\gamma_f}p_m^{\text{in}}, \sqrt{2\gamma_m}x_a^{\text{in}}, \sqrt{2\gamma_m}p_a^{\text{in}}]$. Equation (2) is cast as

$$\frac{du(t)}{dt} = \mathbf{A}u(t) + n(t). \quad (15)$$

The Gaussian steady covariance matrix $V_{ij} = \langle u_i u_j + u_j u_i \rangle$ follows from the equation

$$\mathbf{A}\mathbf{V} + \mathbf{V}\mathbf{A}^T = \mathbf{W}. \quad (16)$$

For low temperatures $T \to 0$, the matrix $\mathbf{W}$ is cast as $\mathbf{W} = \text{diag}(\mathbf{A})$. For the general case, analytic expressions are more involved and the results are presented in Appendix B.

To quantify the magnon-photon entanglement, we use the logarithmic negativity [20,23,36,37]:

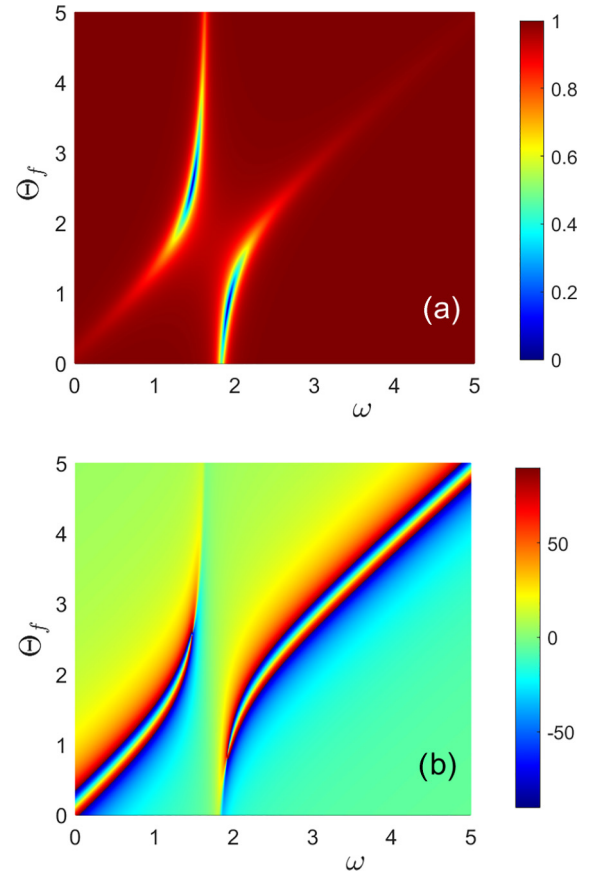$$E_N = \max[0, -\ln[2\eta^-]], \quad (17)$$

FIG. 2. The amplitude (a) $G_0[\Theta_f, \omega]$ and the phase (b) $\phi_g[\Theta_f, \omega]$ of the amplifier [see formulas (2) and (3)] plotted for the values of parameters $\gamma_f = 0.2$, ω_k is given by (4) with $k = \pi/2$, $\gamma_m = 0.04$, $H_0 = 0.2$, and $D_0 = 0.5$. All the quantities are in the reduced units and in graph (b) the color map is in degrees.

where $\eta^- = \min \text{eig}|i\Omega_2 P_{12} V P_{12}|$, $\Omega_2 = \bigoplus_{j=1}^{2} i\sigma_y$, and $P_{12} = \text{diag}(1, -1, 1, 1)$. The entanglement is nonzero (the case of our interest) if $0 < 2\eta^- < 1$. The calculations show that

$$2\eta^- = \sqrt{(\kappa + \delta_0)^2 - 4(\beta_0^2 + \mu^2)} - (\kappa - \delta),$$

$$\kappa = \frac{\gamma_f + \gamma_m}{2\gamma_f}, \quad \beta_0 = \frac{\gamma_m(\omega_k - \omega_f)}{2g\gamma_f}, \quad \mu = \frac{\gamma_m}{2g},$$

$$\delta_0 = \frac{g^2(\gamma_m + \gamma_f) + \gamma_m(\gamma_f^2 + (\omega_k - \omega_f)^2)}{2g^2\gamma_f}. \quad (18)$$

Because of the δ_0 term $2\eta^- > 1$. Thus Eq. (18) reveals that dissipation and decoherence included in the quantum stochastic Langevin equation Eq. (2) leads to a *vanishing steady-state photon-magnon entanglement* for models based on the Hamiltonian $\hat{H}_{\alpha=0}$, given by Eq. (3).

IV. MAGNETOELECTRICALLY INDUCED ENTANGLEMENT

For $\alpha \neq 0$, the cavity electric field in Fig. 1 affects the DMI and hence the magnons. The Hamiltonian $\hat{H}$ for small-
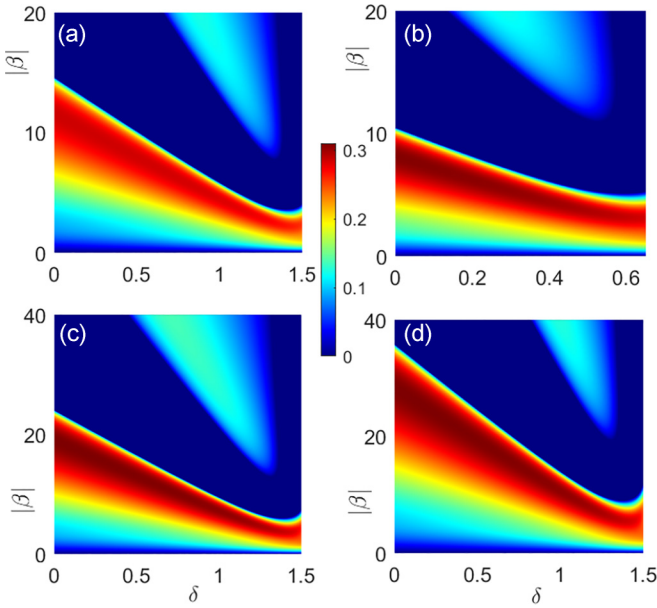
FIG. 3. Logarithmic negativity E_N as a function of the square root of the mean magnon number $|\beta|$, and detuning $\delta = \omega_k - \omega_f$ for the values of parameters $\gamma_m = 0.04$, $\gamma_f = 0.2$. For all graphs, $H_0 = 0.2$, $\Delta_k = \omega_k - \omega_0 = 0$, and $D_0 = 0.3$, while different magnon modes and electric fields are considered: (a) $k = \frac{\pi}{2}$, $D_{0z} = D = 0.05$; (b) $k = \frac{\pi}{4}$, $D_{0z} = D = 0.05$; (c) $k = \frac{\pi}{2}$, $D_{0z} = D = 0.03$; and (d) $k = \frac{\pi}{2}$, $D_{0z} = D = 0.02$.

amplitude spin excitations reads

$$\mathcal{H}_{\text{eff}} = \sum_k \omega_k \hat{m}_k^+ \hat{m}_k + i\mathcal{B}(\hat{m}_k^+ e^{-i\omega_0 t} - \hat{m}_k e^{i\omega_0 t})$$
$$+ \omega_f \hat{a}^+ \hat{a} + iD\hat{m}_k^+ \hat{m}_k(\hat{a} - \hat{a}^+)\sin k. \quad (19)$$

$D = \epsilon U \alpha$ and the magnonic spectrum (4) is modified by the term related to the static electric field along the y axis $D_{0z} = \alpha E_{0y}$

$$\omega_k = H_0 + (1 - \cos k) + (D_0 + D_{0z})\sin k. \quad (20)$$

In contrast to $\hat{H}_{\alpha=0}$ given by Eq. (3), low-energy excitations of the Hamiltonian $\mathcal{H}_{\text{eff}}$, given by Eq. (19), are electromagnons which are governed by nonlinear equation of motion and exhibit electrically controllable electromagnon-photon entanglement. To show this, we insert Eq. (19) in Eq. (2) and write any operator $\hat{Q}$ as $\hat{Q} = \langle Q \rangle + \delta\hat{Q}$, and retain linear terms in the deviation $\delta\hat{Q}$ [25]. Then we obtain a general explicit expression for the entanglement measure (like in $\hat{H}_{\alpha=0}$ case) as $E_N^{h,w} = \max[0, -\ln[2\eta_{h,w}^-]]$. As expected and demonstrated in Appendix A, $E_N^{h,w} \to 0$ for strong damping ($\gamma_f \gg 1$, or $\gamma_f \gg 1$). For further insight, let us adopt the semi-classical approximation $\langle \hat{m}_k^+ \hat{m}_k \rangle = \langle \hat{m}_k^+ \rangle\langle \hat{m}_k \rangle$, $\langle \hat{m}_k^+ \rangle = \beta^* e^{-i\varphi}$, $\langle \hat{m}_k \rangle = \beta e^{i\varphi}$ and consider the resonant case $\Delta_k = \omega_k - \omega_0 = 0$ implying $\beta = \mathcal{B}/\gamma_m$ (cf. Appendix A), with $|\beta|^2$ defines the mean magnon number. For a strong coupling with the classical field, the mean magnon number $|\beta|^2$ is large, approaching the classical limit, i.e., vanishing entanglement as demonstrated by Fig. 3. There, it is shown the entanglement is the largest for vanishing detuning δ and moderate β (or field strength $\mathcal{B}$). For larger detuning, a small entanglement emerges for strong
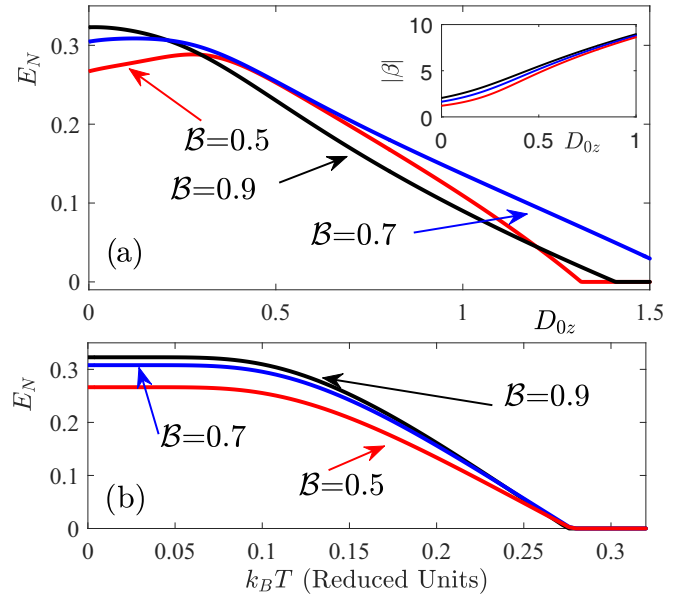

FIG. 4. (a) Dependence of E_N on the external electric field $E_{0y} = D_{0z}/\alpha$ at $T = 0$ for the case $D_0 = 0.3$, $D = 0.05$, $\omega_0 = 1.9$, $\omega_f = 0.5$, and $k = \pi/2$. Inset shows the dependence of the square root of the mean magnon number $|\beta|$ on the external electric field D_{0z}. (b) Dependence of E_N on the bath temperature for the magnonic driving field $\mathcal{B}$. All parameters are the same as in graph (a), and $D_{0z} = 0$.

fields (large β) driven by nonlinearity. Note that we do not consider larger values of δ, since for the given set of parameters, ω_k has a fixed value and we shall keep ω_f positive. On the other hand, for weak fields such that $2\mathcal{B}D \sin k < \gamma_m \omega_f$ we find the limiting expression (cf. Appendix A)

$$E_N^{h,w} = -\ln\left(1 - \frac{2\mathcal{B}D \sin k}{\gamma_m \omega_f}\right). \quad (21)$$

Clearly, the entanglement vanishes at zero field ($\mathcal{B}$) and/or vanishing k vector and/or DMI ($D \to 0$), as illustrated by the results from the formulas in Appendix A, depicted in Fig. 3.

The entanglement E_N can be externally controlled, electrically (via $E_{0y} = D_{z0}/\alpha$) or magnetically, as demonstrated by Fig. 4. As evident from Fig. 4(a), large E_{0y} enhances the mean magnon number $|\beta|^2$. E_N decreases with increasing E_{0y}. This behavior depends on the pumping magnetic field which has an involved role (increases the magnon population and activates nonlinearities). For larger temperatures E_N vanishes but a magnetic field can stabilize to some extent E_N against thermal effects, as demonstrated by Fig. 4(b).

V. DISCUSSIONS AND EXPERIMENTAL PROSPECTS

The aim of this study has been to derive general analytical expressions for a complete class of Hamiltonians that exhibit steady-state entanglement of the low-energy spin excitations to the cavity modes of the electromagnetic field as well as to identify simple expressions for limiting cases that can serve as benchmarks for more numerically based research.

For entanglement measurement we may rely on the following recipe (described in detail in, e.g., Refs. [25,38]):

In essence, independent entries of the Gaussian steady covariance matrix V_{ij} are to be measured [39]. In the experiment, cavity field quadratures are measured directly by homodyning the cavity output. On the other hand, information about the magnon subsystem could be extracted through a weak microwave probe field. We consider the scenario when the entangled photons and magnons have different frequencies $\omega_f \neq \omega_k$. To measure the magnon dynamics, one applies a resonant weak electromagnetic field. The effect of that field on the magnon subsystem is small, and one is left with the first equation from (2) written in the following form: $\frac{da'(t)}{dt} = -i\omega_k a'(t) - D\sin k \langle m_k^+ \rangle \delta m_k - \gamma_f a'(t) + \sqrt{2\gamma_f} a'_{\text{in}}(t)$. As $\langle m_k^+ \rangle = \beta^* e^{-i\varphi}$ and $\delta m_k \propto \exp(i\omega_k t)$, in the rotating frame follows $a'_{\text{out}} = \sqrt{2\gamma_f} a' - a'_{\text{in}} = -\frac{\sqrt{2}D\sin k \langle m_k^+ \rangle \delta m_k}{\gamma_f} + a'_{\text{in}}$. Thus, through measuring the output field, a'_{out} one extracts complete information about the magnonic excitation δm_k.

VI. SUMMARY

As it has been shown above, the magnon-photon entanglement depends on two parameters: the mean magnon number in the cavity $|\beta|^2$ and the detuning between the magnon and the photon modes $\delta = \omega_k - \omega_f$. Different magnon modes are differently entangled with the photons. As general trends, the entanglement is maximal for the resonant modes $\omega_k = \omega_f$ and decays with an increasing mean magnon number in the cavity. For weak D, the maximal magnon-photon entanglement is shifted towards the states with larger magnons [cf. Fig. 3(c)]. While Eq. (21) unveils the entanglement dependence on the cavity field strength, but also a gate voltage (corresponding to E_{0y}) affects the entanglement leading to its decay above a threshold value of E_{0y}. The results point to the potential of other magnetoelectrically active structure such as nanoscale skyrmions [40] and vortices or spin-driven magnetoelectrics [41] (both entails a similar magnonic-magnetoelectric coupling [42–44] as in Eq. (1)). Thereby the strength of the magnetoelectric coupling and the direction of the induced ferroelectric polarization being the determining factors.

APPENDIX A: ABSENCE OF THE STEADY-STATE MAGNON-PHOTON ENTANGLEMENT FOR THE CASE OF ZERO DMI

In the present work, we considered two different Hamiltonians: the model given by Eq. (1), and Eq. (19) containing DMI term, and the model described by Eq. (3) which does not contain DMI term. The Hamiltonian with DMI term Eq. (1) (nonzero α) can be converted into the Hamiltonian without DMI term Eq. (3) through the transformation $\alpha \to 0$, $h_z \to h_y$. As we see from the analytical result in the main text Eq. (21), the steady-state entanglement of the model

stated by Eq. (1), Eq. (19) is not zero when the pumping field $\mathcal{B}$ and the DMI term are not zero $D = \epsilon U \alpha \neq 0$, A nonzero DMI, i.e., nonvanishing $D = \epsilon U \alpha$ is essential for nonzero steady-state magnon-photon entanglement. Without DMI term direct magnon-photon coupling leads to the zero steady-state magnon-photon entanglement, see Refs. [25,35]. These statements are supported by the following. Considering $\alpha = 0$ and exploiting Eqs. (1) and (2) from the main text and in the rotating wave approximation, we deduce the following coupled Heisenberg equations:

$$\frac{d\hat{a}(t)}{dt} = -i\omega_f \hat{a}(t) - ig\hat{m}_k(t) - \gamma_f \hat{a}(t),$$
$$\frac{d\hat{m}_k(t)}{dt} = -i\omega_k \hat{m}_k(t) - i\mathcal{B}e^{-i\omega_0 t} - ig\hat{a}(t) - \gamma_m \hat{m}_k(t). \quad \text{(A1)}$$

After separation of the stationary and perturbation parts of the photonic and magnonic modes $\hat{m}_k(t) = m_k^0 e^{-i\omega_0 t} + \delta\hat{m}_k(t)$, $\hat{a}(t) = a^0 e^{-i\omega_0 t} + \delta\hat{a}(t)$ in the zero approximation, we obtain

$$m_k^0 = \frac{\mathcal{B}(\omega_0 - \omega_f + i\gamma_f)}{(\omega_0 - \omega_k + i\gamma_m)(\omega_0 - \omega_f + i\gamma_f) - g^2},$$
$$a^0 = \frac{\mathcal{B}g}{(\omega_0 - \omega_k + i\gamma_m)(\omega_0 - \omega_f + i\gamma_f) - g^2}. \quad \text{(A2)}$$

For the perturbed parts from Eq. (A1), we obtain the following equations:

$$\frac{d\delta\hat{a}(t)}{dt} = -i\omega_f \delta\hat{a}(t) - ig\delta\hat{m}_k(t) - \gamma_f \delta\hat{a}(t), \quad \text{(A3)}$$
$$\frac{d\delta\hat{m}_k(t)}{dt} = -i\omega_k \delta\hat{m}_k(t) - ig\delta\hat{a}(t) - \gamma_m \delta\hat{m}_k(t).$$

We see that Eq. (A3) can be derived as well through the Hamiltonian $\hat{H}_{\alpha=0}$ Eq. (3) after the substitution $\delta\hat{m}_k(t) \to \hat{m}_k(t)$, and $\delta\hat{a}(t) \to \hat{a}(t)$. Thus, the role of the coherent magnonic pumping field is clear. It causes a shift of the stationary states from zero to nonzero values, as presented in Eq. (A2). However, this is not enough for the nonzero steady-state magnon-photon entanglement in Hamiltonian $\hat{H}_{\alpha=0}$ Eq. (3). According to Eq. (21), for a steady-state magnon-photon entanglement is essential to have a nonzero DMI $\alpha \neq 0$ and for $\alpha \neq 0$ model Eqs. (1) and (19) cannot be converted into model Eq. (3), while in the presence of the magnon pumping field and in the absence of the DMI term Hamiltonians (1) and (3) lead to the same Heisenberg equations.

APPENDIX B: COVARIANCE MATRIX

The next problem is the evaluation of the photon-magnon entanglement for the Hamiltonian $\hat{H}_{\text{eff}}$ [see Eq. (19)] in the presence of dissipation and noise. Using Eq. (2) and Hamiltonian (19) and the commutation relations $[\hat{m}_k, \hat{m}_k^+] = 1$, $\hat{n}_k = \hat{m}_k \hat{m}_k^+$, $[\hat{n}_k, \hat{m}_k] = -\hat{m}_k$, $[\hat{n}_k, \hat{m}_k^+] = \hat{m}_k^+$, $[\hat{a}, \hat{a}^+] = 1$, $\hat{n} = \hat{a}\hat{a}^+$, $[\hat{n}, \hat{a}] = -\hat{a}$, and $[\hat{n}, \hat{a}^+] = \hat{a}^+$, we deduce the set of equations in the rotating wave approximation $\hat{m}_k \to \hat{m}_k e^{-i\omega_0 t}$

and $\hat{m}_{k,\text{in}} \rightarrow \hat{m}_{k,\text{in}} e^{-i\omega_0 t}$:

$$\frac{d\hat{a}}{dt} = -i\omega_f \hat{a} - D\sin(k)\hat{m}_k^+ \hat{m}_k - \gamma_f \hat{a} + \sqrt{2\gamma_f}\hat{a}_{f,\text{in}},$$

$$\frac{d\hat{a}^+}{dt} = i\omega_f \hat{a}^+ - D\sin(k)\hat{m}_k^+ \hat{m}_k - \gamma_f \hat{a}^+ + \sqrt{2\gamma_f}\hat{a}_{f,\text{in}}^+,$$

$$\frac{d\hat{m}_k}{dt} = -i\Delta_k \hat{m}_k + D\sin(k)(\hat{a} - \hat{a}^+)\hat{m}_k - \gamma_m \hat{m}_k$$
$$+ \sqrt{2\gamma_m}\hat{m}_{k,\text{in}} + \mathcal{B},$$

$$\frac{d\hat{m}_k^+}{dt} = i\Delta_k \hat{m}_k^+ + D\sin(k)(\hat{a} - \hat{a}^+)\hat{m}_k^+ - \gamma_m \hat{m}_k^+$$
$$+ \sqrt{2\gamma_m}\hat{m}_{k,\text{in}}^+ + \mathcal{B}. \tag{B1}$$

Here, $\Delta_k = \omega_k - \omega_0$ is the detuning between the external classical magnetic field ω_0 and the magnon frequency ω_k. Introducing the new variables:

$$\hat{x}_m = \frac{\hat{m}_k^+ + \hat{m}_k}{2}, \quad \hat{p}_m = \frac{i(\hat{m}_k^+ - \hat{m}_k)}{2}$$

$$\hat{x}_a = \frac{\hat{a}^+ + \hat{a}}{2}, \quad \text{and} \quad \hat{p}_a = \frac{i(\hat{a}^+ - \hat{a})}{2}, \tag{B2}$$

we rewrite Eq. (B1) above as

$$\frac{d\hat{x}_m}{dt} = \Delta_k \hat{p}_m - \sqrt{2}D\sin(k)\hat{p}_m \hat{p}_a - \gamma_m \hat{x}_m$$
$$+ \sqrt{2\gamma_m}\hat{x}_{m,\text{in}} + \sqrt{2}\mathcal{B},$$

$$\frac{d\hat{p}_m}{dt} = -\Delta_k \hat{x}_m + \sqrt{2}D\sin(k)\hat{x}_m \hat{p}_a - \gamma_m \hat{p}_m$$
$$+ \sqrt{2\gamma_m}\hat{p}_{m,\text{in}} + \sqrt{2}\mathcal{B},$$

$$\frac{d\hat{x}_a}{dt} = \omega_f \hat{p}_a - 2\sin(k)\frac{\hat{x}_m^2 + \hat{p}_m^2 - 1}{2} - \gamma_f \hat{x}_a + \sqrt{2\gamma_f}\hat{x}_{a,\text{in}},$$

$$\frac{d\hat{p}_a}{dt} = -\omega_f \hat{x}_a - \gamma_f \hat{p}_a + \sqrt{2\gamma_f}\hat{p}_{a,\text{in}}. \tag{B3}$$

Following Ref. [25], we use for a general operator $\hat{Q}$ the ansatz: $\hat{Q} = \langle \hat{Q} \rangle + \delta \hat{Q}$, and for the steady state, we exploit the semiclassical approximation $\langle \hat{m}_k^+ \hat{m}_k \rangle = \langle \hat{m}_k^+ \rangle \langle \hat{m}_k \rangle$, $\langle \hat{m}_k^+ \rangle = \beta^* e^{-i\varphi}$, $\langle \hat{m}_k \rangle = \beta e^{i\varphi}$ and deduce $\langle p_m \rangle = \sqrt{2}\beta \sin\varphi$, $\langle x_m \rangle = \sqrt{2}\beta \cos\varphi$, where we assumed that $\sigma = \frac{2\omega_f D^2 \sin^2 k}{\omega_f^2 + \gamma_f^2} <$ 1 is a small parameter. On resonance, i.e., $\Delta_k = \omega_k - \omega_0 = 0$, we infer $\beta = \mathcal{B}/\gamma_m$, $\tan\varphi = \sigma|\beta|^2/\gamma_m$. From the equations of motion, it follows that $\langle p_a \rangle = \frac{\omega_f \sqrt{2}D\sin(k)|\beta|^2}{\omega_f^2 + \gamma_f^2}$ and $\langle x_a \rangle = -\frac{\gamma_f \sqrt{2}D\sin(k)|\beta|^2}{\omega_f^2 + \gamma_f^2}$. Note, $n_\beta \equiv |\beta|^2$ defines the mean magnon number and in the steady state is defined through the following relation:

$$n_\beta \left(\frac{2\omega_f D^2 \sin^2 k}{\omega_f^2 + \gamma_f^2} n_\beta - \Delta_k \right)^2 + n_\beta \gamma_m^2 = \mathcal{B}^2. \tag{B4}$$

In a linear approximation with respect to the perturbations $\delta\hat{x}_m$, $\delta\hat{p}_m$, $\delta\hat{x}_a$, and $\delta\hat{p}_a$, we derive from (B3) the set of equations written in a similar form as Eq. (15) in the main text:

$$\frac{du}{dt} = A_1 u + n, \tag{B5}$$

where $u = (\delta\hat{x}_m, \delta\hat{p}_m, \delta\hat{x}_a, \delta\hat{p}_a)^T$, $n = (\sqrt{2\gamma_m}\delta\hat{x}_{m,\text{in}}, \sqrt{2\gamma_m}\delta\hat{p}_{m,\text{in}}, \sqrt{2\gamma_f}\delta\hat{x}_{a,\text{in}}, \sqrt{2\gamma_f}\delta\hat{p}_{a,\text{in}})$ and the explicit form of the matrix $\mathbf{A}_1$ reads

$$\mathbf{A}_1 = \begin{pmatrix} -\gamma_m & \Delta_k - \sqrt{2}D\langle\hat{p}_a\rangle\sin k & 0 & -\sqrt{2}D\langle\hat{p}_m\rangle\sin k \\ -\Delta_k + \sqrt{2}D\langle\hat{p}_a\rangle\sin k & -\gamma_m & 0 & \sqrt{2}D\langle\hat{x}_m\rangle\sin k \\ -\sqrt{2}D\langle\hat{x}_m\rangle\sin k & -\sqrt{2}D\langle\hat{p}_m\rangle\sin k & -\gamma_f & \omega_f \\ 0 & 0 & -\omega_f & -\gamma_f \end{pmatrix}. \tag{B6}$$

Here, $\omega_k = H_0 + (1 - \cos k) + (D_0 + D_{0z})\sin k$ and $\Delta_k = \omega_k - \omega_0$ is the detuning between the external classical magnetic field ω_0 and the magnon frequency ω_k. We observe that the coupling to the external constant electric field D_{0z} shifts the magnon frequency and deteriorates the resonance condition. However, the effect of the external constant electric field can be compensated for by tuning the frequency of the external classical magnetic field ω_0.

Finally we find the explicit expression for the entanglement as

$$E_N^{h,w} = \max[0, -\ln[2\eta_{h,w}^-]], \tag{B7}$$

with

$$\eta_{h,w}^- = 2^{-1/2}\{\Sigma(V_1) - [\Sigma(V_1)^2 - 4\det V_1]^{1/2}\}^{1/2},$$
$$\Sigma(V_1) = \det G_1 + \det B_1 - 2\det C_1, \tag{B8}$$

and the covariance matrix $\mathbf{V}_1$ is defined as

$$\mathbf{A}_1 \mathbf{V}_1 + \mathbf{V}_1 \mathbf{A}_1^T = \mathbf{W}, \quad \mathbf{V}_1 = \begin{pmatrix} \mathbf{G}_1 & \mathbf{C}_1 \\ \mathbf{C}_1^T & \mathbf{B}_1 \end{pmatrix}. \tag{B9}$$

Choosing the magnon mode $ak = \pi/2$, we show in Fig. 4 in the main text the square root of the mean magnon number $|\beta|$ as a function of D_{0z} for different pumping field values $\mathcal{B}$, see inset of Fig. 4(a). In the limit of weak DMI: $D_0, D_{0z}, D \ll 1$, the steady-state mean magnon number reads $n_\beta = \mathcal{B}^2/(\Delta_k^2 + \gamma_m^2)$. Considering the resonant case $\Delta_k = \omega_k - \omega_0 = 0$ and for a weak DMI, we find upon relatively cumbersome, but otherwise straightforward calculations the expression

$$\eta_{h,w}^- = \frac{1}{2}\left(1 - 2D\sin(k)\frac{\mathcal{B}}{\gamma_m}\frac{1}{\sqrt{(\gamma_m + \gamma_f)^2 + \omega_f^2}}\right). \tag{B10}$$

From Eq. (B10) above and in the limit $\omega_f \gg \gamma_m + \gamma_f$ and $0 < 2\mathcal{B}D\sin(k) < \gamma_m\omega_f$, we obtain the results presented in the main text:

$$E_N^{h,w} = -\ln\left(1 - \frac{2\mathcal{B}D\sin k}{\gamma_m\omega_f}\right). \tag{B11}$$

APPENDIX C: THERMAL ENTANGLEMENT

At finite temperatures, the equation for the thermal covariance matrix takes on the form:

$$A_1 V_1 + V_1 A_1^T = \mathbf{W}, \tag{C1}$$

where A_1 is defined in Eq. (B6) above and the matrix $\mathbf{W}$ has a form

$$\mathbf{W} = -\mathrm{diag}[\gamma_m(2N_m(\omega_k) + 1), \gamma_m(2N_m(\omega_k) + 1), \gamma_f(2N_a(\omega_f) + 1), \gamma_f(2N_a(\omega_f) + 1)]. \tag{C2}$$

Here, $N_a(\omega_f)$ and $N_m(\omega_k)$ are the distribution functions for cavity photons and magnons:

$$N_a(\omega_f) = [\exp[(\hbar\omega_f/k_B T)] - 1]^{-1}, \; N_m(\omega_k) = [\exp[(\hbar\omega_k/k_B T)] - 1]^{-1}. \tag{C3}$$

Therefore the expression of the matrix $\mathbf{W}$ can be rewritten in the compact form:

$$\mathbf{W} = -\mathrm{diag}[\gamma_m \coth[(\hbar\omega_m/2k_B T)], \gamma_m \coth[(\hbar\omega_m/2k_B T)], \gamma_f \coth[(\hbar\omega_f/2k_B T)], \gamma_f \coth[(\hbar\omega_f/2k_B T)]]. \tag{C4}$$

Then the magnon-photon entanglement at a finite temperature is calculated straightforwardly as follows:

$$E_N = \max[0, -\ln 2\eta^-];$$

$$\eta^- = 2^{-1/2}\sqrt{\Sigma(V) - \sqrt{\Sigma(V)^2 - 4\det V}};$$

$$\Sigma(V) = \frac{1}{4}\coth^2\left(\frac{\hbar\omega_m}{2k_B T}\right) + \frac{1}{4}\coth^2\left(\frac{\hbar\omega_f}{2k_B T}\right) + 2\left(\frac{D\sin(k)\mathcal{B}}{\gamma_m}\right)^2 \frac{1}{\left((\gamma_m + \gamma_f)^2 + \omega_f^2\right)}\coth\left(\frac{\hbar\omega_m}{2k_B T}\right)\coth\left(\frac{\hbar\omega_f}{2k_B T}\right);$$

$$\Sigma(V)^2 - 4\det V = \frac{1}{16}\left[\coth^2\left(\frac{\hbar\omega_m}{2k_B T}\right) - \coth^2\left(\frac{\hbar\omega_f}{2k_B T}\right)\right]^4 + 2\left(\frac{D\sin(k)\mathcal{B}}{\gamma_m}\right)^2$$
$$\times \frac{1}{\left((\gamma_m + \gamma_f)^2 + \omega_f^2\right)}\coth\left(\frac{\hbar\omega_m}{2k_B T}\right)\coth\left(\frac{\hbar\omega_f}{2k_B T}\right)\left[\coth^2\left(\frac{\hbar\omega_m}{2k_B T}\right) + \coth^2\left(\frac{\hbar\omega_f}{2k_B T}\right)\right]; \tag{C5}$$

In the low-temperature case,

$$k_B T \ll \hbar\omega_m, \hbar\omega_f, \; \coth\left(\frac{\hbar\omega_m}{2k_B T}\right) = 1, \; \coth\left(\frac{\hbar\omega_f}{2k_B T}\right) = 1, \tag{C6}$$

we find Eq. (B10) above. Concerning the microscopic theory and the crucial role of electronic correlation and spin-orbital interaction in determining the magnetoelectric coupled, we refer to the works [45,46].

[1] Y. Chougale, J. Talukdar, T. Ramos, and R. Nath, Dynamics of Rydberg excitations and quantum correlations in an atomic array coupled to a photonic crystal waveguide, Phys. Rev. A **102**, 022816 (2020).

[2] M. Manzoni, L. Mathey, and D. Chang, Designing exotic many-body states of atomic spin and motion in photonic crystals, Nat. Commun. **8**, 1 (2017).

[3] A. Goban, C. Hung, S. Yu, J. Hood, J. Muniz, J. Lee, M. Martin, A. McClung, K. Choi, and D. Chang, Others Atom–light interactions in photonic crystals, Nat. Commun. **5**, 3808 (2014).

[4] C. Hung, S. Meenehan, D. Chang, O. Painter, and H. Kimble, Trapped atoms in one-dimensional photonic crystals, New J. Phys. **15**, 083026 (2013).

[5] J. Douglas, H. Habibian, C. Hung, A. Gorshkov, H. Kimble, and D. Chang, Quantum many-body models with cold atoms coupled to photonic crystals, Nat. Photonics **9**, 326 (2015).

[6] D. Lachance-Quirion, Y. Tabuchi, A. Gloppe, K. Usami, and Y. Nakamura, Hybrid quantum systems based on magnonics, Appl. Phys. Express **12**, 070101 (2019).

[7] H. Huebl, C. Zollitsch, J. Lotze, F. Hocke, M. Greifenstein, A. Marx, R. Gross, and S. Goennenwein, High Cooperativity in Coupled Microwave Resonator Ferrimagnetic Insulator Hybrids, Phys. Rev. Lett. **111**, 127003 (2013).

[8] Y. Tabuchi, S. Ishino, T. Ishikawa, R. Yamazaki, K. Usami, and Y. Nakamura, Hybridizing Ferromagnetic Magnons and Microwave Photons in the Quantum Limit, Phys. Rev. Lett. **113**, 083603 (2014).

[9] X. Zhang, C. Zou, L. Jiang, and H. Tang, Strongly Coupled Magnons and Cavity Microwave Photons, Phys. Rev. Lett. **113**, 156401 (2014).

[10] J. Haigh, N. Lambert, A. Doherty, and A. Ferguson, Dispersive readout of ferromagnetic resonance for strongly coupled

magnons and microwave photons, Phys. Rev. B **91**, 104410 (2015).

[11] M. Aspelmeyer, T. Kippenberg, and F. Marquardt, Cavity optomechanics, Rev. Mod. Phys. **86**, 1391 (2014).

[12] Y. Cao, P. Yan, H. Huebl, S. Goennenwein, and G. Bauer, Exchange magnon-polaritons in microwave cavities, Phys. Rev. B **91**, 094423 (2015).

[13] B. Zare Rameshti, Y. Cao, and G. Bauer, Magnetic spheres in microwave cavities, Phys. Rev. B **91**, 214430 (2015).

[14] L. Bai, M. Harder, Y. Chen, X. Fan, J. Xiao, and C. Hu, Spin Pumping in Electrodynamically Coupled Magnon-Photon Systems, Phys. Rev. Lett. **114**, 227201 (2015).

[15] S. Viola Kusminskiy, H. Tang, and F. Marquardt, Coupled spin-light dynamics in cavity optomagnonics, Phys. Rev. A **94**, 033821 (2016).

[16] Ö. Soykal, and M. Flatté, Strong Field Interactions between a Nanomagnet and a Photonic Cavity, Phys. Rev. Lett. **104**, 077202 (2010).

[17] X. Zhang, T. Liu, M. Flatté, and H. Tang, Electric-Field Coupling to Spin Waves in a Centrosymmetric Ferrite, Phys. Rev. Lett. **113**, 037202 (2014).

[18] L. Abdurakhimov, S. Khan, N. Panjwani, J. Breeze, M. Mochizuki, S. Seki, Y. Tokura, J. Morton, and H. Kurebayashi, Magnon-photon coupling in the noncollinear magnetic insulator, Phys. Rev. B **99**, 140401 (2019).

[19] Y. Li, W. Zhang, V. Tyberkevych, W. Kwok, A. Hoffmann, and V. Novosad, Hybrid magnonics: Physics, circuits, and applications for coherent information processing, J. Appl. Phys. **128**, 130902 (2020).

[20] R. Simon, Peres-Horodecki Separability Criterion for Continuous Variable Systems, Phys. Rev. Lett. **84**, 2726 (2000).

[21] L. Duan, G. Giedke, J. Cirac, and P. Zoller, Inseparability Criterion for Continuous Variable Systems, Phys. Rev. Lett. **84**, 2722 (2000).

[22] M. Hillery, and M. Zubairy, Entanglement Conditions for Two-Mode States, Phys. Rev. Lett. **96**, 050503 (2006).

[23] G. Adesso, and F. Illuminati, Entanglement in continuous-variable systems: recent advances and current perspectives, J. Phys. A: Math. Theor. **40**, 7821 (2007).

[24] Q. He, P. Drummond, M. Olsen, and M. Reid, Einstein-Podolsky-Rosen entanglement and steering in two-well Bose-Einstein-condensate ground states, Phys. Rev. A **86**, 023626 (2012).

[25] J. Li, S. Zhu, and G. Agarwal, Magnon-Photon-Phonon Entanglement in Cavity Magnomechanics, Phys. Rev. Lett. **121**, 203601 (2018).

[26] H. Yang, O. Boulle, V. Cros, A. Fert, and M. Chshiev, Controlling Dzyaloshinskii-Moriya interaction via chirality dependent atomic-layer stacking, insulator capping and electric field, Sci. Rep. **8**, 12356 (2018).

[27] W. Zhang, H. Zhong, R. Zang, Y. Zhang, S. Yu, G. Han, G. Liu, S. Yan, S. Kang, and L. Mei, Electrical field enhanced interfacial Dzyaloshinskii-Moriya interaction in MgO/Fe/Pt system, Appl. Phys. Lett. **113**, 122406 (2018).

[28] S. Tiablikov, *Methods in the Quantum Theory of Magnetism* (Springer, New York, 2013).

[29] D. Walls and G. Milburn, *Quantum Optics* (Springer Science and Business Media, New York, 2007).

[30] C. Gardiner, and M. Collett, Input and output in damped quantum systems: Quantum stochastic differential equations and the master equation, Phys. Rev. A **31**, 3761 (1985).

[31] B. Chen, H. Xing, J. Chen, H. Xue, and L. Xing, Tunable fast–slow light conversion based on optomechanically induced absorption in a hybrid atom–optomechanical system, Quant. Info. Proc. **20**, 1 (2021).

[32] P. Wahl, P. Simon, L. Diekhoner, V. Stepanyuk, P. Bruno, M. Schneider, and K. Kern, Exchange Interaction between Single Magnetic Adatoms, Phys. Rev. Lett. **98**, 056601 (2007).

[33] D. Maroulakos, L. Chotorlishvili, D. Schulz, and J. Berakdar, Local and Non-Local Invasive Measurements on Two Quantum Spins Coupled via Nanomechanical Oscillations, Symmetry **12**, 1078 (2020).

[34] H. Yuan, P. Yan, S. Zheng, Q. He, K. Xia, and M. Yung, Steady Bell State Generation via Magnon-Photon Coupling, Phys. Rev. Lett. **124**, 053602 (2020).

[35] H. Yuan, S. Zheng, Z. Ficek, Q. He, and M. Yung, Enhancement of magnon-magnon entanglement inside a cavity, Phys. Rev. B **101**, 014419 (2020).

[36] G. Vidal, and R. Werner, Computable measure of entanglement, Phys. Rev. A **65**, 032314 (2002).

[37] M. Plenio, Logarithmic Negativity: A Full Entanglement Monotone That is not Convex, Phys. Rev. Lett. **95**, 090503 (2005).

[38] D. Vitali, S. Gigan, A. Ferreira, H. Böhm, P. Tombesi, A. Guerreiro, V. Vedral, A. Zeilinger, and M. Aspelmeyer, Optomechanical Entanglement between a Movable Mirror and a Cavity Field, Phys. Rev. Lett. **98**, 030405 (2007).

[39] J. Laurat, G. Keller, J. Oliveira-Huguenin, C. Fabre, T. Coudreau, A. Serafini, G. Adesso, and F. Illuminati, Entanglement of two-mode Gaussian states: characterization and experimental production and manipulation, J. Opt. B: Quantum Semiclassical Opt. **7**, S577 (2005).

[40] R. Wiesendanger, Nanoscale magnetic skyrmions in metallic films and multilayers: a new twist for spintronics, Nature Rev. Mat. **1**, 16044 (2016).

[41] M. Fiebig, T. Lottermoser, D. Meier, and M. Trassin, The evolution of multiferroics, Nature Rev. Mat. **1**, 16046 (2016).

[42] V. Jandieri, R. Khomeriki, L. Chotorlishvili, K. Watanabe, D. Erni, D. Werner, and J. Berakdar, Photonic Signatures of Spin-Driven Ferroelectricity in Multiferroic Dielectric Oxides, Phys. Rev. Lett. **127**, 127601 (2021).

[43] X. Wang, L. Chotorlishvili, V. Dugaev, A. Ernst, I. Maznichenko, N. Arnold, C. Jia, J. Berakdar, I. Mertig, and J. Barnaś, The optical tweezer of skyrmions, npj Comput. Mater. **6**, 140 (2020).

[44] D. Yu, C. Sui, D. Schulz, J. Berakdar, and C. Jia, Nanoscale Near-Field Steering of Magnetic Vortices, Phys. Rev. Appl. **16**, 034032 (2021).

[45] H. Katsura, N. Nagaosa, and A. Balatsky, Spin Current and Magnetoelectric Effect in Noncollinear Magnets, Phys. Rev. Lett. **95**, 057205 (2005).

[46] T. Liu, and G. Vignale, Electric Control of Spin Currents and Spin-Wave Logic, Phys. Rev. Lett. **106**, 247203 (2011).